AD-A063 195 SMITHSONIAN ASTROPHYSICAL OBSERVATORY CAMBRIDGE MASS F/G 3/2
MODELS FOR SOLAR CORONAL HOLES.(U)
SEP 78 G L WITHBROE
UNCLASSIFIED F19628-76-C-0281
AFGL-TR-78-0217 NL

| OF |
AD A
063195

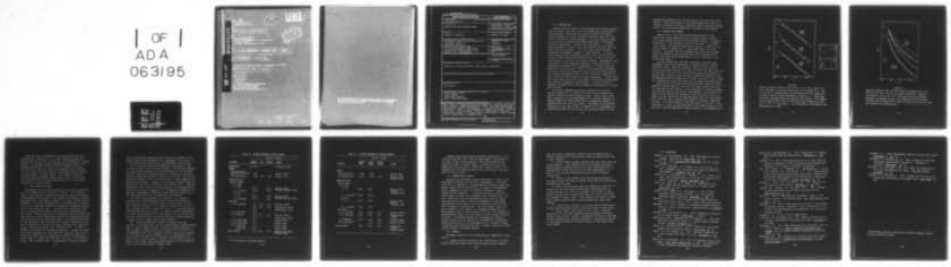

END
DATE
FILMED
3 -79
DDC

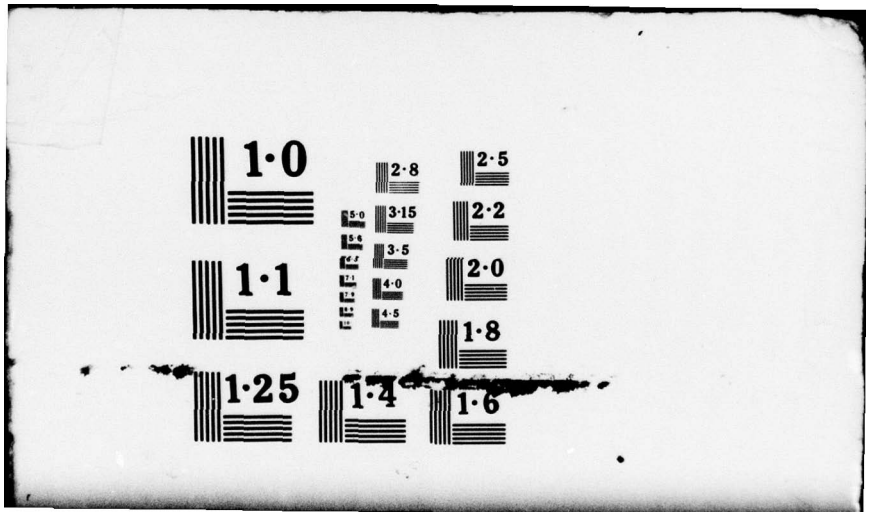
1·0
1·1
1·25
1·4
1·6
1·8
2·0
2·2
2·5
2·8
3·15
3·5
4·0
4·5
5·0

LEVEL II

(18) (19) AFGL-TR-78-0217

(12)

(6) MODELS FOR SOLAR CORONAL HOLES.

(10) George L. Withbroe
Smithsonian Astrophysical Observatory
60 Garden Street
Cambridge, Massachusetts 02138

(9) Final Report, [redacted] 1 Aug [redacted] 76 - 31 Jul [redacted] 78,

(11) 30 Sep [redacted] 78 (12) 20p.

Approved for public release; distribution unlimited

(15) F19628-76-C-0281

(16) 4643

(17) 03

AIR FORCE GEOPHYSICS LABORATORY
AIR FORCE SYSTEMS COMMAND
UNITED STATES AIR FORCE
HANSCOM AFB, MASSACHUSETTS 01731

044 850

79 01 12 006

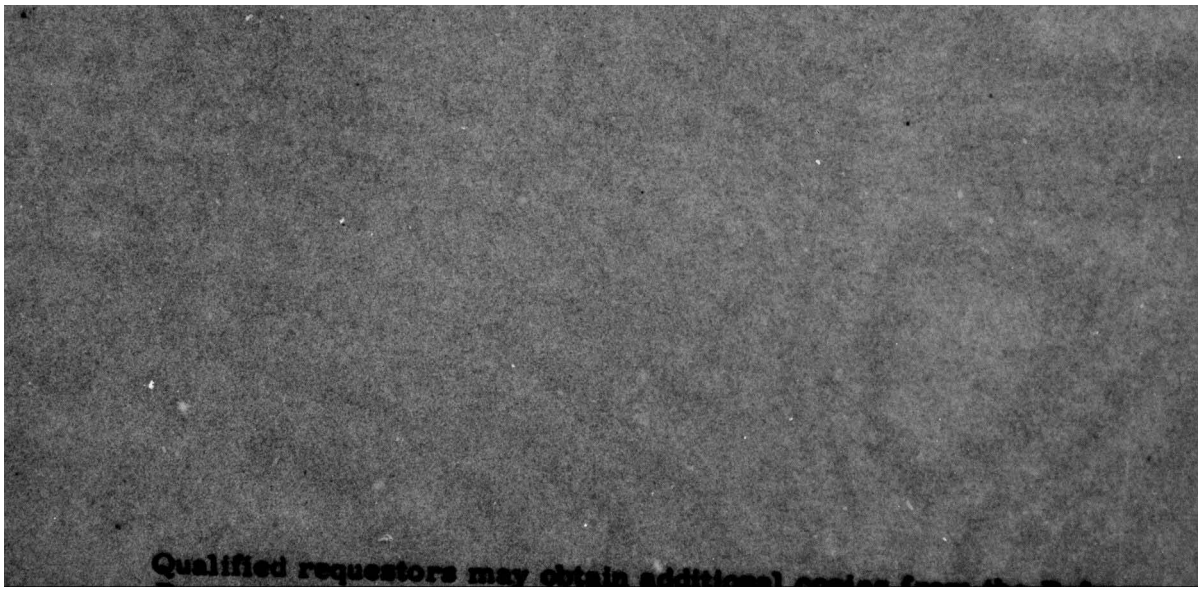
Qualified requestors may obtain additional

Unclassified

SECURITY CLASSIFICATION OF THIS PAGE (When Data Entered)

REPORT DOCUMENTATION PAGE		READ INSTRUCTIONS BEFORE COMPLETING FORM
1. REPORT NUMBER AFGL-TR-78-0217	2. GOVT ACCESSION NO.	3. RECIPIENT'S CATALOG NUMBER
4. TITLE (and Subtitle) MODELS FOR SOLAR CORONAL HOLES		5. TYPE OF REPORT & PERIOD COVERED Scientific. Final 1 Aug 1976-31 July 1978
		6. PERFORMING ORG. REPORT NUMBER
7. AUTHOR(s) George L. Withbroe		8. CONTRACT OR GRANT NUMBER(s) F19628-76-C-0281
9. PERFORMING ORGANIZATION NAME AND ADDRESS Smithsonian Astrophysical Observatory 60 Garden Street Cambridge, MA 02138		10. PROGRAM ELEMENT, PROJECT, TASK AREA & WORK UNIT NUMBERS 62101F 46430302
11. CONTROLLING OFFICE NAME AND ADDRESS Air Force Geophysics Laboratory Hanscom AFB, Massachusetts 01731 Monitor/ D.A. Guidice/PHP		12. REPORT DATE 30 September 1978
		13. NUMBER OF PAGES 20
14. MONITORING AGENCY NAME & ADDRESS(if different from Controlling Office)		15. SECURITY CLASS. (of this report) Unclassified
		15a. DECLASSIFICATION/DOWNGRADING SCHEDULE

16. DISTRIBUTION STATEMENT (of this Report)

Approved for public release; distribution unlimited.

17. DISTRIBUTION STATEMENT (of the abstract entered in Block 20, if different from Report)

18. SUPPLEMENTARY NOTES

Tech Other

19. KEY WORDS (Continue on reverse side if necessary and identify by block number)

Solar Coronal Holes
Solar Corona
Solar Quiet Regions
Solar Transition Layer

20. ABSTRACT (Continue on reverse side if necessary and identify by block number)

This report summarizes several investigations of coronal holes and quiet regions. Temperature-density models for those regions have been derived from EUV observations. It is found that the coronal temperature, density, and temperature gradient are lower in coronal holes than in quiet regions. There is evidence for a positive temperature gradient to heights of 0.3 solar radii in quiet regions and 2.5 solar radii in coronal holes.

DD FORM 1 JAN 73 1473 EDITION OF 1 NOV 65 IS OBSOLETE

Unclassified

SECURITY CLASSIFICATION OF THIS PAGE (When Data Entered)

1.0 INTRODUCTION

Coronal holes are areas on the sun where the coronal temperature and density are lower than the surrounding quiet areas and active regions. These features appear as regions of greatly reduced emission in coronal extreme ultraviolet (EUV) and X-ray lines, as regions of low brightness in the white light K-corona, and as regions of reduced brightness temperature at decimeter and meter wavelengths. Coronal holes also appear to be areas where the magnetic field is open and therefore regions where the solar wind can originate. It is the latter factor that has generated considerable interest in these features. In recent years there has been increasing evidence that coronal holes are a major source, perhaps the primary source, of the solar wind, particularly the recurrent high-speed streams. Consequently, the investigation of the physical conditions in coronal holes is of fundamental importance to the development of reliable physical models for the solar wind. There are also implications regarding solar terrestrial relations, because the solar wind provides one of the mechanisms by which the sun influences conditions in the terrestrial magnetosphere and upper atmosphere. Coronal holes have been identified as the long sought for M-regions responsible for recurrent geomagnetic disturbances. A recent review by Withbroe and Noyes (1977) gives a number of references to coronal hole studies.

This report summarizes several investigations into the physical conditions in coronal holes that were performed with support of AFGL contract F19628-76-C-0281. These studies have been concerned with the development of an improved temperature-density model for coronal holes and for comparison purposes, an improved model for the quiet corona. Knowledge of the physical conditions in the lower corona is needed for the development of theoretical models for the corona and the specification of the

mechanisms responsible for coronal heating and solar wind acceleration. Since the results of the above studies have been presented in published scientific papers and AFGL scientific reports, we will give only brief summaries of the work in this report.

2.0 CORONAL HOLE MODELS

Mariska (1977, 1978) has utilized observations of the intensities of EUV emission lines to derive empirical models for a polar coronal hole and the surrounding corona. A complete description of the analysis is given in the papers by Mariska (1977, 1978). The EUV data were used to derive a model for the lower corona to a height of 0.2 solar radii above the solar surface. This model was then extended out to four solar radii above the surface by Munro and Mariska (1977) through use of Skylab and ground based measurements of the brightness of the white light corona.

The EUV observations utilized in Mariska's analysis were obtained by the Harvard experiment on Skylab (Reeves, Timothy, and Huber, 1977). Emission gradient curves for EUV emission lines of lithium-like ions O VI λ1032, Ne VIII λ770, Mg X λ625, Al XI λ550 and Si XII λ521 were derived from spectroheliograms of a coronal hole located at the north pole during the summer of 1973. The measured emission gradients are given in Figures 1 and 2 along with theoretical curves calculated for the model discussed below.

Since the line of sight along which the EUV intensities were measured contains material from both the polar coronal hole and the surrounding quiet corona, it was necessary to construct models for both the coronal hole and its surroundings. The boundary between the two regions was assumed to have the form $\Theta=a(\rho-\rho_o)+\Theta_o$, where Θ is the angle that the boundary makes with the solar north pole along the line of sight which passes a distance ρ (measured in units of a solar radius $R_\odot$) from the center of the disc. The constants a, Θ_o and ρ_o were determined to be respectively, 65, 23° and 0.92. For the temperature density models it was assumed that

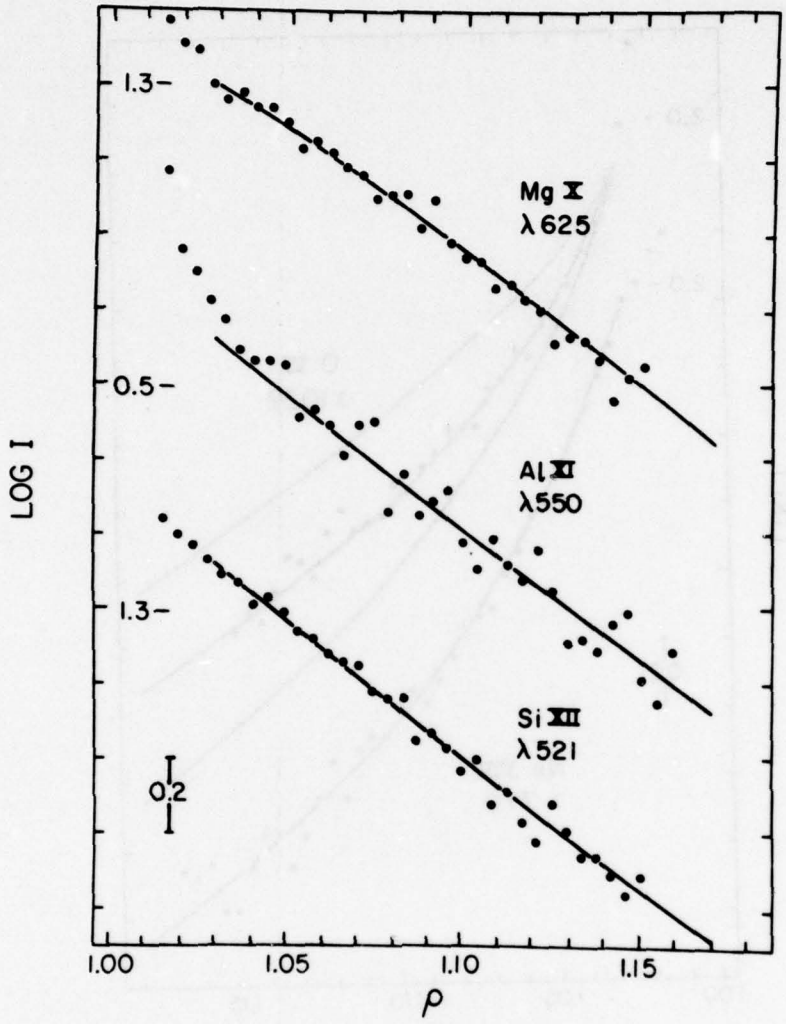

Figure 1

Emission gradient data for Mg X λ625, Al XI λ550, and Si XII λ521 observed at the solar north pole on 14 August 1973. The points are the observations and the curves are the predicted emission from the model discussed in Section 2.0. Each curve has been displaced along the ordinate for clarity. The number to the left of each curve is the log of the intensity in erg cm^{-2} s^{-1} sr^{-1} at that point. The divisions on the ordinate are separated by 0.2 dex.

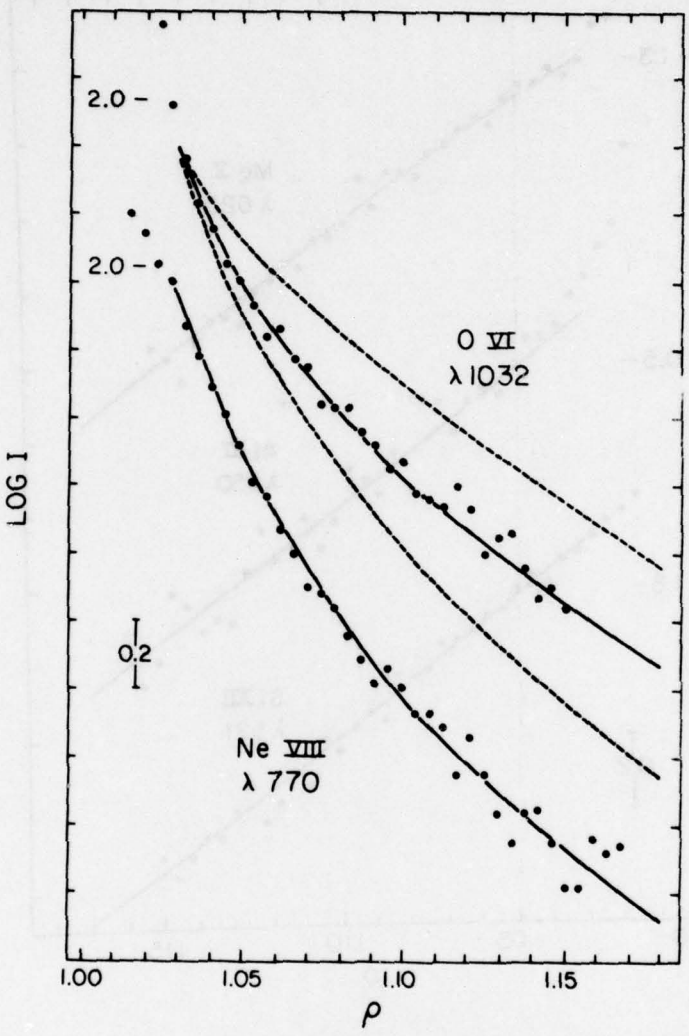

Figure 2

Emission gradient data and the predicted emission for O VI λ1032 and Ne VIII λ770 for the region detailed in Figure 1. The dashed lines on the O VI λ1032 data are the predicted emission from models in which the conductive flux has been increased and decreased by a factor of two from the value that best matches the observations.

the corona is in hydrostatic equilibrium, a good approximation in the low corona even if mass flows of the order of 10-20 km/sec are present. The corona surrounding the coronal hole could be represented by an isothermal model characterized by a temperature of 2×10^6 K and electron density 3.1×10^8 cm^{-3} at a height of 36,400 km. The model for the coronal hole is characterized by an electron density of 1.7×10^8 cm^{-3} at 0.03 $R_\odot$ above the surface, a constant downward directed conductive flux of 6×10^4 $erg/cm^2/sec$ and coronal temperature of 1.1×10^6 K reached at a height of 0.08 $R_\odot$. The above models are applicable to the lower corona for heights up to about 0.2 $R_\odot$ above the surface. Emission gradients calculated from the above models are given in Figures 1 and 2.

The values of the coronal temperature and density obtained by Mariska are in good agreement with those obtained in earlier EUV coronal hole studies (Munro and Withbroe, 1972; Withbroe and Wang, 1972). The value of the conductive flux is a factor of 1.7 less than the values found in earlier studies. The new determination of the conductive flux is particularly important, because it is the first determination of the conductive flux in a coronal hole that is independent of the assumed densities. Instead it depends upon the shape of the emission gradient curves, which can be determined to a much higher precision with the Skylab data than with earlier measurements made with lower spatial resolution. The density distribution determined for this polar coronal hole is close to the minimum polar density distribution tabulated by Allen (1973).

Munro and Mariska (1977) combined the above results with white light observations to produce an empirical self-consistent coronal hole model between the base of the corona (height of approximately 0.05 $R_\odot$) and 4. $R_\odot$ above the surface. A smooth density distribution was found to match the EUV data and white light data from the HAO 1973 ground-based eclipse expedition and Skylab experiment. By assuming the outward flow of polar coronal material into the solar wind is similar to that in high speed solar wind streams measured at 1 astronomical unit, Munro and

Mariska determined the velocity and pressure distribution within the coronal hole present at the north solar pole in the summer of 1973 (cf. Munro and Jackson, 1977). In the absence of accelerating forces other than those due to gravity and gas pressure, the derived kinetic temperature of the plasma (about 10^6K at the base of the corona) is consistent with the EUV observations and increases outward from the sun to heights at least 2.5 $R_\odot$ above the surface. This implies that material is being heated and/or momentum is being transferred to the plasma (e.g. by wave-particle interactions) to this height. Under the above assumptions the coronal temperature at a height of 2.5 $R_\odot$ may exceed $3x10^6$K in the coronal hole. Most of the solar wind acceleration also occurs at this height range with the velocity increasing from about 10 km/sec at a height of 0.1 $R_\odot$, to 100 km/sec at 0.6 $R_\odot$ to 500 km/sec at 4 $R_\odot$. The coronal hole geometry found by Munro and Mariska is shown in Figure 3. This figure illustrates that the angular area of the coronal hole increases by nearly an order of magnitude between the solar surface and a distance 5 $R_\odot$ from sun center. The model based on the combined EUV and white light data is not consistent with measurements of radio brightness temperatures at frequencies below 100 MHz (e.g. Dulk et al. 1977). This suggests the possibility that the difficulties encountered by Dulk et al. in obtaining a self-consistent coronal hole model from EUV and radio data may result from systematic errors in the absolute calibration of the relevant radio measurements.

3.0 INHOMOGENEITIES IN CORONAL HOLES

One of the major types of inhomogeneities in polar coronal holes are polar plumes. These are ray-like coronal structures observed in polar regions in EUV, X-ray and white light observations. These features appear to overlie coronal bright points observed in EUV and X-ray coronal lines. Ahmad and Withbroe (1977) utilized EUV observations of three polar plumes to construct

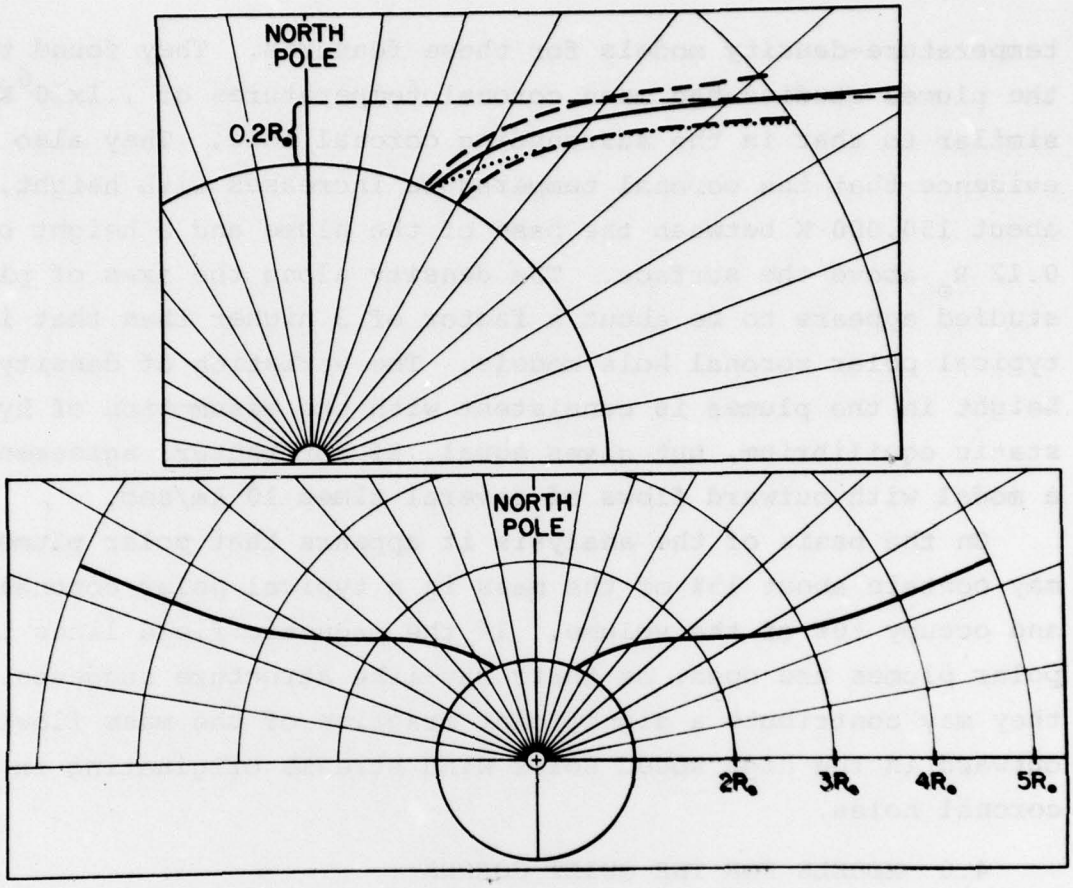

Figure 3

Polar Hole Boundary. It was shown by Munro and Jackson (1977) that the polar hole was essentially axisymmetric about the north pole during the summer of 1973. Minor changes in the location of this boundary near the solar surface occurred between the times when the eclipse data (30 June) and the EUV data (14 August) were obtained. These changes are shown in the top portion of the figure. The dotted line depicts the Munro and Jackson boundary on 2 July. The lower and upper dashed lines represent boundaries on 7 and 21 August respectively -- indicating that the shape of the hole was undergoing modification during the EUV observations on 14 August. The assumed boundary for the combined observations is denoted by the solid line; the entire boundary from the solar surface to 5 $R_\odot$ is shown in the bottom portion of the figure.

temperature-density models for these features. They found that the plumes studied had mean coronal temperatures of 1.1×10^6 K, similar to that in the surrounding coronal hole. They also found evidence that the coronal temperature increases with height, by about 150,000 K between the base of the plume and a height of 0.12 $R_\odot$ above the surface. The density along the axes of plumes studied appears to be about a factor of 3 higher than that in typical polar coronal hole models. The variation of density with height in the plumes is consistent with the assumption of hydrostatic equilibrium, but gives equal, if not better, agreement to a model with outward flows of several times 10 km/sec.

On the basis of the analysis it appears that polar plumes may contain about 15% of the mass in a typical polar coronal hole and occupy 10% of the volume. If the magnetic field lines in polar plumes are open, as their ray-like structure suggests, they may contribute a significant fraction of the mass flowing outward in the high speed solar wind streams originating in coronal holes.

4.0 MODELS FOR THE QUIET CORONA

Mariska and Withbroe (1978) have utilized emission gradients derived from Skylab measurements of intensities of EUV emission lines in typical quiet regions to determine densities and temperature gradients in the quiet corona. Their analysis suggests that the coronal temperature rises throughout the height range 0.03 $R_\odot$ to 0.3 $R_\odot$ above the surface. This result implies that in quiet regions there is significant coronal heating beyond 0.3 $R_\odot$ above the surface. The density distribution determined for the quiet-sun model is consistent with the mean density structure of the inner corona determined by Saito (1970) from a large body of eclipse and white light K-coronameter observations. The EUV observations, coupled with Saito's results, appear to be most consistent with a coronal temperature which increases from between 1.6 and 1.8 million degrees at a height 0.05 $R_\odot$ to between 2.5 and 3 million degrees at a height of 0.4 $R_\odot$. These temperatures

are significantly higher than those in the polar coronal hole model, by about 600,000 K at a height of 0.08 $R_\odot$. A representative value for the downward conductive flux is about 2×10^5 erg/cm^2/sec, larger than that in the polar coronal hole by a factor of about 3. The density at 0.03 $R_\odot$ is about a factor of 2 higher than in the polar coronal hole.

5.0 CORONAL ENERGY BALANCE

Mariska (1977) has used the above models for typical quiet regions and polar coronal hole to determine the coronal energy losses due to thermal conduction and radiation. These values are given in Table I. The other major energy loss is the solar wind. In his study Mariska used the solar wind losses for coronal holes, 6.4×10^5 erg/cm^2/sec, estimated by Bame *et al.* (1977) who assumed that all of the solar wind flux originates in coronal holes that cover 20% of the solar surface. This estimate is in good agreement with that of Withbroe and Noyes (1977), 7×10^5 erg/cm^2/sec, determined by using typical densities and velocities for high-speed streams which were assumed to originate in coronal holes whose angular area increases by a factor of 6 between the solar surface and distances far above the surface. If some portion of the average solar wind originates in normal quiet regions, then the mean coronal energy loss due to the solar wind escaping from quiet regions must be equal to or less than about 10^5 erg/cm^2/sec (Mariska 1977; Withbroe & Noyes 1977).

Table I Coronal Energy Losses

	Quiet Region	Coronal Hole
Conductive flux	2×10^5	6×10^4
Radiative flux	5×10^4	9×10^3
Solar wind flux	10^5	6×10^5
Total coronal loss	3×10^5	7×10^5

Note: All fluxes are in units of erg/cm^2/sec at the solar surface.

Since the above estimates for the total energy loss are uncertain by a factor of 2 to 3, these estimates suggest the possibility that the total energy loss, and therefore the coronal heating, is the same in quiet regions and coronal holes. This suggests the possibility that one way to measure the energy carried away in the solar wind is by measuring some parameter in coronal holes that will reflect the lowered coronal temperature and density in these regions. For example, decimetric or metric radio brightness temperatures in coronal holes may be correlated with the energy carried away by the solar wind originating in these regions.

6.0 THE TRANSITION LAYER

Knowledge of the physical conditions in the solar transition region is important for a variety of reasons. The transition layer is the interface through which mass and energy flow between the chromosphere and corona. The transport of energy by thermal conduction into the transition layer is a primary coronal cooling mechanism. A reliable determination of the magnitude of energy lost by this mechanism depends on knowledge of temperature gradients in the transition layer. This layer may also play a major role in determining the mass flow between the chromosphere and the corona. Current empirical and theoretical models suggest that there may be a unique relationship between the temperature gradient and density in the transition layer, a relationship specified by the requirement that the mechanical energy, radiative and conductive fluxes be in balance (cf. Moore and Fung 1972; McWhirter et al. 1975; Rosner et al. 1977; Withbroe 1978). In order to achieve this balance the atmosphere responds to changes in mechanical energy deposition in the transition layer and corona by increasing or decreasing the temperature gradients and densities in these layers (cf. Moore and Fung 1972; Pye et al. 1977; Rosner et al. 1977; Withbroe 1978). Consequently, it appears possible

that the transition layer not only acts as an interface in the flow of mass and energy between the chromosphere and corona, but it also exerts some control over the magnitude of these flows.

One of the most difficult parameters to determine for the transition layer is the electron pressure. The electron pressure is a more useful parameter for many purposes than the electron density, because the electron pressure is expected to be nearly constant across the transition layer due to the fact that the geometrical thickness of the transition layer is small compared to a pressure scale height. Tables II and III give electron pressures derived by a variety of techniques (see Withbroe 1977). Table II demonstrates that within the uncertainties of the determinations, typically ± 0.3 dex, it appears to be a reasonable assumption that the quiet chromosphere, transition layer and lower corona have the same pressure and are in hydrostatic equilibrium.

One of the major problems yet remaining in the study of coronal holes is determining whether the electron pressure in the transition layer of coronal holes is nearly equal to that in quiet regions or whether it is lower by a factor of 2 to 3 as would be expected if the transition layer is in pressure equilibrium with the overlying corona. It has been firmly established in studies described earlier in this report and in previous work that the coronal layers of coronal holes have electron pressures a factor of 2 to 3 lower than in quiet regions.

The results presented in Table III suggest that the pressure in the transition layer of coronal holes is approximately equal to that in quiet regions. Since the emission measures in the two types of regions are nearly identical for $4.5 < \log T < 5.9$ (see Withbroe 1977), this suggests that the temperature gradient in the transition layer of coronal holes is approximately the same as that in quiet regions. Because of the possible implications in the energy, mass and pressure balance in the transition layer, these results require further study.

TABLE II. ELECTRON PRESSURES IN QUIET REGIONS

TECHNIQUE	Log P/k = log $N_e T$ AVERAGE	CELL	NETWORK	SOURCE
CHROMOSPHERE	14.7-14.9			Vernazza (1977b)
CORONA				
Limb Observations (White light and EUV)	14.8			Mariska (1977)
Disk Observations	14.9	14.9	14.9	Mariska (1977)
TRANSITION LAYER				
Optical Depths*				
C II λ1335				
(ξ = 0)	$\gtrsim$14.2		$\gtrsim$14.3	Mariska (1977); Withbroe, Mariska (1976)
(ξ = 17 km/sec)	$\gtrsim$13.8		$\gtrsim$14.0	
C III λ977				
(ξ = 0)	$\gtrsim$14.5		$\gtrsim$14.7	Mariska (1977); Withbroe, Mariska (1976)
(ξ = 17 km/sec)	$\gtrsim$14.2		$\gtrsim$14.4	
Line Ratios				
C III λ1176/λ977	14.9	14.6	15.1	Vernazza (1977a)
	14.6	14.5	14.6	Dupree et al. (1977)
	14.4			Dufton et al. (1977)
N III λ772/λ989	14.5			
O V λ760/λ630	14.9	14.3	15.1	Vernazza (1977a)
	14.4			Dufton et al. (1977)
C III λ1247/λ1908	15.1			Nicolas (1977)
Si III λ1301/λ1296	15.3			Nicolas (1977)
O IV λ1404/λ1401	15.2			Nicolas (1977)
λ1407/λ1404	15.2			Nicolas (1977)
Energy Balance	14.5	14.3	14.7	Rosner et al. (1977); Withbroe (1977b)

* ξ is the assumed microturbulent velocity

TABLE III. ELECTRON PRESSURES IN DIFFERENT REGIONS

TECHNIQUE	Log P/k = log $N_e T$ CORONAL HOLE	QUIET REGION	ACTIVE REGION	SOURCE
CORONA				
Limb Observations	14.40	14.80		Mariska (1977)
Disk Observations	14.45	14.90	15.6	Mariska (1977); Withbroe (1977)
TRANSITION LAYER				
Optical Depths				
C II λ1335				
(ξ = 0)	$\gtrsim$14.2	$\gtrsim$14.2		Mariska (1977); Withbroe, Mariska (1976)
(ξ = 17 km/sec)	$\gtrsim$13.8	$\gtrsim$13.8		
C III λ977				
(ξ = 0)	$\gtrsim$14.1	$\gtrsim$14.5		Mariska (1977); Withbroe, Mariska (1976)
(ξ = 17 km/sec)	$\gtrsim$13.8	$\gtrsim$14.2		
Line Ratios				
C III λ1175/λ977	14.9	14.9	15.5	Vernazza (1977a)
N III λ772/λ989	14.5	14.5	15.1	Vernazza, Mason (1977)
O V λ760/λ629	14.9	14.9	15.8	Vernazza (1977a)
Mg IX λ439/λ368		14.5	15.0	Vernazza (1977a)
Energy Balance	14.4	14.5	15.5	Rosner et al. (1977); Withbroe (1977b)

Another result that requires further investigation is the finding by Mariska (1977) that spicules appear to contribute of the order of 60% of the emission in EUV lines formed in the transition layer of coronal holes. If this result should be supported in future work, it would have a major effect on our conceptions of the mass and energy flow in the lower transition layer of coronal holes.

7.0 CHROMOSPHERIC MODELS

We have also performed a significant amount of work on the development of models for the quiet chromosphere. This work, which will be reported in a future paper by Vernazza, Avrett and Loeser, deals with the derivation of a series of chromospheric models representing areas of different brightness in quiet regions of the atmosphere. If additional work on transition region models confirms the hypothesis that the densities in the lower transition layer are approximately the same in coronal holes and quiet regions, then the chromospheric models being developed for quiet regions can be utilized for coronal holes with a minimum of modifications. The final models, which are nearly complete, will consist of a homogenous model for the chromospheric layer in quiet regions and a set of six models for representative network and cell areas in quiet regions and coronal holes. Differences between the chromospheric layers in coronal holes and quiet regions are accounted for by assigning different fractions of the chromospheric area to each of these six models, since coronal holes have a smaller fraction of bright network elements than quiet regions.

8.0 SUMMARY

The major findings in the investigations summarized in this report:

1) Models derived from Skylab EUV observations of a polar coronal hole and typical quiet region confirm earlier results

that the coronal temperature, density and the energy loss by thermal conduction are significantly lower in coronal holes than in quiet regions.

2) Coronal models derived from EUV and white light data are self-consistent. This suggests that the discrepancies found between models developed from EUV and radio data may be due to uncertainties in the analysis of the radio measurements, or errors in the absolute calibration of the radio brightness temperatures.

3) There is some evidence that the electron pressures in the lower transition layer in coronal holes and quiet regions are approximately the same.

4) There are significant positive temperature gradients in the corona, with the coronal temperature increasing with increasing height to at least 0.3 $R_\odot$ above the surface in quiet regions and possibly to heights as high as 2.5 $R_\odot$ or more above the surface in coronal holes. This implies that there is significant coronal heating and/or momentum deposition above these heights.

5) A significant fraction of the solar wind acceleration in coronal holes may occur within a few solar radii of the surface.

6) Polar plumes, which appear to be coronal structures associated with the small magnetic bipolar regions underlying coronal bright points, contain a significant fraction of the mass in polar coronal holes and may contribute a significant fraction of the plasma flowing out of these regions in high speed solar wind streams.

9.0 REFERENCES

*Ahmad, I.A. and Withbroe, G.L. 1977, "EUV Analysis of Polar Plumes", AFGL-TR-0167; Solar Phys. 53, 397.

Allen, C.W. 1973, Astrophysical Quantities (3rd ed; London: Athlone), p. 176.

Bame, S.J., Asbridge, J.K., Feldman, W.C. and Gosling, J.T. 1977, "Evidence for a Structure-free State at High Solar Wind Speeds", J. Geophys. Res. 82, 1487.

Dufton, P.L., Berrington, K.A., Burke, P.G. and Kingston, A.E. 1978, "The Interpretation of C III and O V Emission Line Ratios in the Sun", Astron. Astrophys. 62, 111.

Dulk, G.A., Sheridan, K.V., Smerd, S.F. and Withbroe, G.L. 1977, "Radio and EUV Observations of a Coronal Hole", Solar Phys. 52, 349.

Dupree, A.K., Foukal, P.V. and Jordan, C. 1977, "Plasma Diagnostic Techniques in the UV: The C III Density-Sensitive Lines in the Sun", Astrophys. J. 209, 621.

*Mariska, J.T. 1977, "The Structure of the Solar Transition Region and Inner Corona", Ph.D. Thesis, Harvard University.

*Mariska, J.T. 1978, "Analysis of Extreme Ultraviolet Observations of a Polar Coronal Hole", AFGL-TR-77-0187; Astrophys. J., 225, 252.

*Mariska, J.T. and Withbroe, G.L. 1978, "Temperature Gradients in the Inner Corona", Solar Phys., in press.

McWhirter, R.W.P., Thonemann, P.C. and Wilson, R. 1975, "The Heating of the Solar Corona II. A Model Based on Energy Balance", Astron. Astrophys. 40, 63.

Moore, R.L. and Fung, P.C.W. 1972, "Structure of the Chromosphere-Corona Transition Region", Solar Phys. 23, 78.

Munro, R.H. and Jackson, B.V. 1977, "Physical Properties of a Polar Coronal Hole from 2 to 5 $R_{\odot}$", Astrophys. J. 213, 874.

*Munro, R.H. and Mariska, J.T. 1977, "A Composite Coronal Hole Model", Bull. Amer. Astron. Soc. 9, 360. Also presented at OSO-8 Workshop, University of Colorado, Boulder.

Munro, R.H. and Withbroe, G.L. 1972, "Properties of a Coronal Hole Derived from EUV Observations", Astrophys. J., 176, 511.

Nicolas, K.R. 1977, "The Application of Si III Line Intensity Ratios to Determine the Solar Transition Zone Density and Pressure", Ph.D. Thesis, University of Maryland.

Pye, J.P., Evans, K.P., Hutcheon, R.J., Gerassimenko, M., Davis, J.M., Krieger, A.S., and Vesecky, J.F. 1977, "The Structure of the X-ray Bright Corona above Active Region McMath 12628 and Derived Implications for the Description of Equilibria in the Solar Atmosphere", Astron. Astrophys. 65, 123.

Rosner, R., Tucker, W.H. and Vaiana, G.S. 1978, "Dynamics of the Quiescent Solar Corona", Astrophys. J. 220, 643.

Reeves, E.M., Timothy, J.G. and Huber, M.C.E. 1977, "Extreme UV Spectroheliometer on the Apollo Telescope Mount", Applied Optics, 16, 837.

Saito, K. 1970, "A Non-spherical Axisymmetric Model of the Solar K-corona of the Minimum Type", Ann. Tokyo Astron. Obs., Ser. 2, 12, 53.

*Vernazza, J.E. 1977a, "Density-Sensitive Lines in the Extreme Ultraviolet Region", presented at IAU Colloquium No. 43 on UV and X-ray Spectroscopy of Astrophysical and Laboratory Plasmas, London.

*Vernazza, J.E. 1977b, private communication.

*Vernazza, J.E. and Mason, H.E. 1978, "Density Sensitivity of the Solar EUV Emission from Boron-like Ions", Astrophys. J., in press.

*Withbroe, G.L. 1977, "The Chromosphere and Transition Layer in Coronal Holes", in Coronal Holes and High Speed Wind Streams, ed. J.B. Zirker (Colorado Associated University Press), p. 145.

*Withbroe, G.L. 1977, "Models for the Solar Transition Layer", AFGL-TR-78-0067; Proceedings of the November 7-10 1977 OSO-8 Workshop, p. 2.

Withbroe, G.L. 1978, "The Thermal Phase of a Large Solar Flare", Astrophys. J., 225, 641.

Withbroe, G.L. and Mariska, J.T. 1976, "Analysis of EUV Limb Brightening Observations from ATM II: Influence of Spicules", Solar Phys. 48, 21.

*Withbroe, G.L. and Noyes, R.W. 1977, "Mass and Energy Flow in the Solar Chromosphere and Corona", Ann. Rev. Astron. Astrophys. 15, 363.

Withbroe, G.L. and Wang, Y. 1972, "A Model for the Polar Transition Layer and Corona for November 1967", Solar Phys. 27, 394.

*Publications resulting from total or partial support of AFGL contract F19628-76-C-0281.